



Title	Adsorption states of NO on the Pt(111) step surface
Author(s)	Tsukahara, N.; Mukai, K.; Yamashita, Y.; Yoshinobu, J.; Aizawa, H.
Citation	Surface Science, 600(17), 3477-3483 https://doi.org/10.1016/j.susc.2006.06.040
Issue Date	2006-09-01
Doc URL	http://hdl.handle.net/2115/15877
Type	article (author version)
File Information	SurfaceS600-17.pdf



[Instructions for use](#)

Adsorption states of NO on the Pt(111) step surface

N. Tsukahara K. Mukai Y. Yamashita J. Yoshinobu*

*The Institute for Solid State Physics, University of Tokyo, 5-1-5 Kashiwanoha,
Kashiwa, Chiba, 277-8581, Japan*

H. Aizawa

*Creative Research Initiative "Sousei", University of Hokkaido, N21W10 Kita-ku,
Sapporo, Hokkaido, 001-0021, Japan*

Abstract

Using infrared reflection absorption spectroscopy (IRAS) and scanning tunneling microscopy (STM), we investigated the adsorption states of NO on the Pt(997) step surface. At 90 K, we observed three N-O stretching modes at 1490 cm^{-1} , 1631 cm^{-1} and 1700 cm^{-1} at 0.2 ML. The 1490 cm^{-1} and 1700 cm^{-1} peaks were assigned to NO molecules at fcc-hollow and on-top sites of the terrace, respectively. The 1631 cm^{-1} peak was assigned to the step NO species. In the present STM results, we observed that NO molecules were adsorbed at the bridge sites of the step as well as fcc-hollow and on-top sites of the terrace. To help with our assignments, density functional theory calculations were also performed. The calculated results indicated that a bridge site of the step is the most stable adsorption site for NO, and its stretching frequency was 1607 cm^{-1} . The interactions between NO species at different sites on Pt(997) are also discussed.

Key words:

Platinum; Steps ; Nitrogen monoxide ; Adsorption ; Infrared reflection absorption spectroscopy ; Scanning tunneling microscopy ; Density functional calculations

* Corresponding author. Tel.:+81-4-7136-3320 ; Fax:+81-4-7136-3474
Email address: yoshinobu@issp.u-tokyo.ac.jp (J. Yoshinobu).

1 Introduction

The adsorption and reaction of nitric monoxide (NO) on transition metal surfaces are important from industrial, environmental, and scientific viewpoints. The unpaired electron in the antibonding 2π orbital of NO increases the variety of surface reactions as compared to the case of CO. So far many studies have been carried out to determine the adsorption states of NO on metal surfaces [1].

The adsorption states of NO on the Pt(111) surface were studied using several experimental techniques. Using electron energy loss spectroscopy (EELS) and infrared reflection absorption spectroscopy (IRAS), 1490 cm^{-1} and 1690 cm^{-1} peaks were observed at low and high coverages at 100 K, respectively. Ibach and Lehwald concluded that NO adsorbed as a monomer at low coverage, and with increasing coverage NO molecules adsorbed as dimer species near the saturation coverage [2]. Gland and Sexton [3] and Hayden [4] proposed an adsorption model based on the comparison of the stretching vibrational energy of the adsorbed NO with that of NO in nitrosyl complexes. In their model, NO adsorbs at a two-fold bridge site at low coverage and switches to an on-top site as the coverage increases. On the other hand, Kiskinova et al. found an O 1s peak at 530.6 eV, which was assigned to NO on a bridge site at low coverage, and a second peak at 532.5 eV which was assigned to the on-top NO at high coverage. At the saturation coverage, only one broad peak at 531.1 eV was observed, which was assigned to disordered NO [5]. The transition from the bridge to the on-top sites, as suggested from EELS and IRAS results [3,4] does not agree with the XPS results.

On the contrary, using dynamical low energy electron diffraction (LEED), Materer et al. reported that at 0.25 ML the p(2×2) NO fcc-hollow site model gave the best fit between LEED experiment and calculation. (1 ML is defined as one adsorbate molecule per surface atom) [6,7]. Ge and King calculated the adsorption energies of NO on Pt(111) based on density functional theory (DFT) with generalized gradient approximation (GGA) [8]; and they also found that the fcc-hollow site was the most stable site for NO.

Recently, the adsorption states of NO on Pt(111) have been studied in detail [9-14]. Using dynamical LEED analysis, with the aid of scanning tunneling microscopy (STM) and high resolution EELS, Matsumoto et al. investigated the adsorbed states of NO on Pt(111) as a function of coverage. First, NO molecules are adsorbed at fcc-hollow sites up to 0.25 ML and form the p(2×2) ordered structure. Next, NO is additionally adsorbed at on-top sites up to 0.5 ML. Finally up to saturation coverage (0.75 ML), NO occupied fcc-, hcp-hollow and on-top sites [9-11]. By the latest DFT calculation, Aizawa et al. also supported these results [12]. Furthermore, they have calculated the peak

intensities (i.e. square dynamic dipole moments) and the wavenumbers of N-O stretching vibrations as a function of the coverage.

Real metal surfaces contain various defects, such as steps and kinks, and thus adsorption states become more complex than those on a flat surface. Since molecules often interact strongly with the defect sites, the defects on the surface have a strong influence on chemical reactions on inhomogeneous surfaces [15,16]. Thus, as a model of defect surfaces, it is important to study surface chemical reactions on well-defined step surfaces.

Recently, using temperature programmed desorption (TPD), Sugisawa et al. [17] and Mukerji et al. [18] found that NO was dissociated at the step on Pt(211) above 230 K and then N₂ and N₂O were observed as desorption products. In addition, Mukerji et al. studied the adsorption states of NO on Pt(211) using DFT calculation and IRAS [19]. They reported that NO adsorbed at a bridge site of the step and its stretching energy was 1620 cm⁻¹ at 120 K; at 307 K NO-O complexes were formed and the absorption band was observed at 1801 cm⁻¹. Backus et al. reported similar results for NO on Pt(533) using TPD, IRAS and DFT calculations [20]. However, so far there is no direct experimental evidence that NO adsorbs at a bridge site of the step.

In this study, we have investigated the adsorption states of NO molecules on the Pt(997) surface at low temperature, using IRAS and STM. The DFT calculation was performed to evaluate the adsorbed states of NO on Pt(553).

2 Experiments and calculations

The Pt(997) surface has a periodic step-terrace structure; miscutting about 6.5° from the [111] direction. The terrace of this surface has a (111) close-packed structure constituted by 9 rows of Pt atoms, and the monoatomic step is formed by a (111) microfacet.

The IRAS and STM experiments were carried out in an ultrahigh vacuum chamber. The base pressure of the chamber was less than 1×10^{-10} Torr. The Pt(997) clean surface was carefully prepared by repeated cycles of 800 eV Ne-ion sputtering and annealing at 800 K, and repeated cycles of oxidation under 1×10^{-7} Torr O₂ and flashing to 1300 K in the preparation chamber. The sample was transferred to the main chamber in which the sample holder was connected to a liquid He/liquid N₂ reservoir and surrounded by triple thermal shields. Gaseous NO molecules at room temperature were introduced to the cold sample surface through a pulse gas dosing system, at an angle of about 45° from the surface normal direction. With constant pressure in the gas line and a constant duration for opening the valve, the exposure was accurately

controlled by the number of shots.

First-principles calculations were performed for NO molecules adsorbed on the Pt(553) surface. The Pt(553) surface is similar to the Pt(997) surface in the sense that both surfaces consist of (111) terraces and (111) monoatomic steps. The only difference is in the width of the terrace; the Pt(997) surface involves 9 atom wide terraces, while on the Pt(553) surface the terrace is only 5 atom wide. We consider that the calculations for the Pt(553) surface reproduce the essential features of chemical processes taking place on the Pt(997) surface, because from a chemical perspective the steps usually play a much more important role than terraces.

All the calculations were carried out using a program called STATE, which has been successfully applied to both metal and semiconductor surfaces [25]. The calculations were based upon the DFT with GGA. The PBE-type exchange-correlation functional was employed [26]. Only valence electrons (5d and 6s for Pt, and 2s and 2p for N and O) were treated explicitly. Ultrasoft pseudopotentials [27] were used for the N 2p, O 2p, and Pt 5d states, while norm-conserving pseudopotentials [28] were used for the other states. Wavefunctions were expanded by plane waves, whose cutoff energy was taken to be 30.25 Ry. The number of k-points can be small, as the size of the unit cell is large in the present calculations. We adopted a two-dimensional 2x2 uniform k-point mesh. We used a slab consisting of an NO molecule layer and 15 Pt layers. The NO molecule layer, as well as the upper 10 Pt layers, were allowed to relax in geometrical optimization procedures. The surface unit cell contains one step and one terrace consisting of 5 atomic rows. The periodicity parallel to the step was set to be 3 atoms. Spin-polarization effect was not taken into account, because most previous calculations of NO on transition-metal surfaces have indicated that chemisorbed NO is not spin-polarized [29].

3 Results & discussion

3.1 IRAS measurements of NO adsorption on Pt(997) at 90 K

IRAS spectra of NO on Pt(997) at 90 K are shown in Fig. 1 as a function of NO exposure. When the valve of the gas line was opened once (= 1 shot), a certain amount of NO gas was introduced onto the Pt(997) clean surface; the coverage of NO on Pt(997) was about 0.02 ML at this condition. At low coverage (Fig. 1 (a)), two peaks were observed at 1484 cm^{-1} and 1630 cm^{-1} , respectively. With increasing NO exposure (Fig. 1 (b),(c) and (d)), another peak appeared at 1700 cm^{-1} , and the intensity of the 1484 cm^{-1} peak decreased. In addition, their line shapes became asymmetric. Moreover, a small peak at 1615 cm^{-1} was

also observed. At saturation coverage (Fig. 1 (e)), four peaks were observed at 1713, 1632, 1504 and around 1440 cm^{-1} ; the peak intensity at 1632 cm^{-1} decreased.

The peaks at 1700 cm^{-1} and 1484 cm^{-1} are assigned to N-O stretching modes at on-top and threefold fcc-hollow sites on the (111) terrace, respectively [10,12]. Similar peaks were observed in the previous IRAS studies of NO on Pt(111) [11,21,22] and Pt(533) [20].

The peak at 1630 cm^{-1} was not observed in the previous vibrational studies of NO on the Pt(111) flat surface. Therefore this peak should originate from the presence of the step, that is, an N-O stretching mode of NO adsorbed at a step site. In the previous studies of NO on Pt(211), the peak at about 1620 cm^{-1} was assigned to the N-O stretching mode at a bridge site of the step based on DFT calculations [18-20]. Here the peak at 1630 cm^{-1} in Fig.1 is tentatively assigned to the N-O stretching mode at the bridge site of the step, which will be discussed in detail later, based on the present STM results.

The peak intensity at 1484 cm^{-1} grew with increasing NO coverage, and its frequency blue-shifted to 1492 cm^{-1} . This shift was due to a dipole-dipole coupling between the NO molecules at the fcc-hollow sites [21,23]. When the peak at 1700 cm^{-1} appeared, the peak intensity at 1484 cm^{-1} began to decrease and the frequency red-shifted. In the previous vibrational experiments of NO on Pt(111) [10,11] and Pt(533) [20], the intensity decrease and the red-shift to 1484 cm^{-1} were observed with the existence of NO at the on-top site. In the DFT calculation of NO on Pt(111) [12], its dynamic dipole moment at the fcc-hollow site decreased as the coverage increased from 0.25 ML to 0.5 ML. It was suggested that this was caused by intensity transfer as a result of dipole-dipole interaction [23], and in addition, by a change in the electronic structure of the entire adsorbed system with increasing coverage [12]. With increasing NO coverage in the range from 0.25 ML to 0.5 ML (these states correspond to spectra from (b) to (d) in Fig. 1.), a broad peak appears in the range from 1420 to 1460 cm^{-1} . This may be assigned to the N-O stretching mode at the fcc-hollow site, red-shifted by co-adsorption of on-top species [10-12].

The decrease of the peak intensity at 1632 cm^{-1} was observed at high coverage. Besides, the peak at 1615 cm^{-1} gradually developed (Fig. 1 (d)). This may be due to the hollow NO on the terrace. The small peak at 1504 cm^{-1} (Fig. 1 (e)) is assigned to an N-O stretching mode at a threefold hcp-hollow site [10-12]. This behavior was also observed in the case of NO on Pt(111) at the saturation coverage [10,11,21].

3.2 IRAS measurements of NO adsorption on Pt(997) at 140 K

IRAS spectra of NO on Pt(997) at 140 K are shown in Fig. 2 as a function of NO exposure. At this condition, the coverage of NO on Pt(997) by one shot of NO gas injection was about 0.01 ML. At low coverage (Fig. 2 (a) and (b)), only one peak appeared at 1630 cm^{-1} and developed with the blue-shift to 1634 cm^{-1} (Fig. 2 (b)). With increasing NO exposure, a peak at 1481 cm^{-1} and absorption band in the range from 1700 cm^{-1} to 1800 cm^{-1} additionally appeared (Fig. 2 (c)). When the peak at 1481 cm^{-1} appeared, the peak intensity at 1634 cm^{-1} decreased and another peak was newly observed at 1615 cm^{-1} . At 43 shots (Fig. 2 (d)), the peak frequency at 1481 cm^{-1} shifted to 1495 cm^{-1} and its intensity increased. In addition, another peak appeared at 1705 cm^{-1} . At 55 shots (Fig. 2 (e)), the peak frequency at 1705 cm^{-1} shifted to 1709 cm^{-1} and its intensity increased. Here, the peak at 1495 cm^{-1} decreased in intensity and red-shifted to about 1450 cm^{-1} . At 70 shots (Fig. 2 (f)), a small peak at 1505 cm^{-1} appeared, and the decrease of the peak intensity at 1633 cm^{-1} was observed. In addition, the peak at 1709 cm^{-1} become bimodal containing peaks of 1710 and 1725 cm^{-1} . At 80 shots (Fig. 2 (g)), the Pt(997) surface was saturated with chemisorbed NO molecules.

Since the surface migration of NO on the terrace is thermally activated at 140 K, all NO molecules adsorb at the step in the low coverage region (Fig. 2 (a) and (b)). Therefore this site is the most stable for NO on Pt(997). We already reported this fact by the heating experiment in the previous IRAS study of NO on Pt(997) [31]. Note that the step is the most stable adsorption site for CO on Pt(997) [24].

After the step species at 1634 cm^{-1} were saturated in intensity, NO started to adsorb at fcc-hollow sites of the terrace. We think that NO molecules at the terrace influence those at the step, as in the case of the fcc-hollow species and the on-top species on Pt(111) [10-12,20,21]. As a result of the interaction, change in the local electronic structure occurs and the peak of the step NO molecules splits into two peaks at 1633 cm^{-1} and 1615 cm^{-1} , respectively. The same peak split was observed at 90 K. Note that NO at a hollow site distorted the Pt atoms underneath itself in previous dynamical LEED studies and the DFT calculation of NO on Pt(111) [6-8,11]. In our previous IRAS measurement of NO on Pt(997) at 11 K [31], the peak due to step NO species appeared at 1615 cm^{-1} , and shifted to 1630 cm^{-1} after heating. At 11 K, thermal diffusion is quenched and more NO molecules stay on the terrace than those at 90 K. Therefore, substrate Pt atoms at 11 K are more affected by adsorbed NO molecules compared to those at 90 K, and thus the peak of step NO species appear not at 1630 cm^{-1} but at 1615 cm^{-1} . However, not all step NO species shifted to 1615 cm^{-1} at 90 K. This is related to the position of hollow NO species and will be discussed in the next section with STM images.

In addition, an absorption band in the range from 1700 cm^{-1} to 1800 cm^{-1} appeared. An absorption band of around 1750 cm^{-1} could be due to NO molecules at on-top sites of the step. In the previous IRAS studies of NO on Pt(110) [32,33], a broad peak at 1758 cm^{-1} was observed at high coverage and the peak at 1626 cm^{-1} decreased coincidentally. The 1626 cm^{-1} peak originates from bridge NO species on the Pt row of Pt(110). The 1758 cm^{-1} peak is assigned to on-top species under the existence of bridge NO species on the same row at high coverage. This behavior is very similar to the present case discussed below.

At 90 K, NO molecules on the terrace do not fully migrate, and some NO molecules stay on the terrace in this low coverage region. Thus, the step sites are not saturated and some NO molecules form the local $p(2\times 2)$ structure on the terrace. The $p(2\times 2)$ structure is energetically stable and NO in the $p(2\times 2)$ island may not migrate to the step site. On the other hand at 140 K (Fig. 2 (b) and (c)), half of the bridge sites at steps are occupied, and additional NO on the terrace can migrate to a step site. When additional NO arrives at a step, the local coverage at the step increases and the site occupation of on-top sites also occurs; the local coverage at the step becomes more than 0.5.

In Fig. 2 (d) and (e), the peak intensity of the fcc-hollow species decreased, but the on-top species increased in intensity. However, the peak intensity of the step species did not change significantly. Thus, the on-top species of the terrace do not interact significantly with the step bridge species in this coverage region.

At high coverage (Fig. 2 (f) and (g)), the peak of hcp-hollow species appeared at 1505 cm^{-1} [10,11,21]. The spectrum at the saturation coverage shows similar adsorption states to that at 90 K; fcc-hollow, on-top and hcp-hollow sites of the terrace, and the bridge and on-top sites of the step are occupied. In addition, the bimodal broad peak is observed at 1709 cm^{-1} . This is due to the existence of on-top species on the terrace and the step, as discussed above.

3.3 STM measurement of NO adsorption on Pt(997) at 86 K

An STM image of NO on Pt(997) at 86 K is shown in Fig. 3. The sample bias (V_s) and the tunnel current (I_t) were -0.1 V and 0.2 nA, respectively. In this condition, NO molecules were observed as bright protrusions [9,10]. The coverage of NO molecules was directly estimated by counting the number of bright spots; it is about 0.2 ML in Fig. 3. The close-up image of the rectangle in Fig. 3 and the registry map are shown in Fig. 4 (a) and (b), respectively. Note that an IRAS spectrum corresponding to this condition is shown in Fig. 1(b). That spectrum indicates that NO molecules adsorb at fcc-hollow sites of the terrace (1490 cm^{-1}) and bridge sites of the step (1631 cm^{-1}), and begin to

adsorb at on-top sites of the terrace (1700 cm^{-1}). Three adsorption states of NO on Pt(997) were also observed in this STM image; two are on the terrace and the other is at the step. As compared with the IRAS spectrum, the less bright one on the terrace is assigned to the NO molecule at the fcc-hollow site, and the brighter one at the center of three fcc-hollow NO molecules is assigned to NO at the on-top site (1700 cm^{-1}) [9,10].

On the terrace, NO molecules at the fcc-hollow site and the on-top site form the hexagonal structure. The nearest-neighbor distance between two NO molecules at the same kind of adsorption site is about 0.55 nm. Therefore NO molecules on the terrace form a $p(2\times 2)$ structure similar to the case of NO on Pt(111). These assignments of NO at the fcc-hollow site and the on-top site agree with the previous STM study of NO on Pt(111) [9,10].

We determined the adsorption site of NO at the step judging from the adsorption sites of NO on the (111) terrace [9,10]. By using a registry mesh, as shown in Fig. 4 (a), we conclude that NO on the step adsorbs at a bridge site. The nearest-neighbor distance between NO molecules at the step is also about 0.55 nm. Therefore NO molecules at bridge sites are located in the period of twice the Pt nearest-neighbor distance (0.277 nm).

Fig. 4(b) shows the adsorption model for an STM image in Fig. 4(a). Using site adsorption model, we can explain the split of the peak at 1630 cm^{-1} in IRAS spectra in Figs. 1 and 2. A nearest-neighbor NO of a bridge NO on the step is located either at the hollow site or at the on-top site; a singleton NO at the step also exists. As discussed in the previous section, NO molecules on the step significantly interact with those at the hollow site of the terrace. Therefore, if the nearest-neighbor NO of a step NO is located at the hollow, the N-O frequency at the step species is changed. In contrast, the peak shift due to the adsorption at the on-top site on the terrace is smaller.

3.4 DFT calculations of NO on Pt(553)

In order to elucidate the adsorption states of NO of the stepped Pt(111) surface, we conducted the DFT calculation of NO on Pt(553). By geometrical optimization procedures, we found a number of adsorption geometries of NO on the Pt(553) surface, which correspond to energy local minima in the potential energy surface. The calculated results for the cases in which the NO molecule is adsorbed near the step are shown in Table 1 and Fig. 5 (a)-(f). As can be seen from Table 1, the bridge site at the step is the most stable adsorption site (with an adsorption energy of 2.49 eV), which is consistent with the discussions based on the IRAS and STM data in the previous sections. The calculated N-O stretching frequency for this adsorption site is 1607 cm^{-1} ,

which is in good agreement with the experimental value of about 1630 cm^{-1} . Note that the adsorption of NO at the bridge site on the (111) terrace does not give a local minimum of the potential energy surface and is thus unstable [12]. The bridge-site adsorption can be attained only in the presence of step.

It is interesting to compare the adsorption energies near the step with that in the middle of the (111) terrace. Let us take the fcc-hollow site, for example. The adsorption energy at the fcc-hollow site in the middle of the terrace was calculated to be 1.94 eV [30]. The adsorption energies at the fcc-hollow site on the upper and lower terraces near the step are 2.15 and 1.62 eV, respectively, as shown in Table 1. It seems that adsorption sites near the step on the upper terrace are more stable than the corresponding sites in the middle of the terrace. Therefore, when the surface temperature is raised and NO molecules become mobile, they tend to be adsorbed at sites near the step on the upper terrace.

In Fig. 2, the IRAS spectra for 70 and 80 shots exhibit a large bimodal peak around 1715 cm^{-1} . This peak probably consists of the on-top species on the terrace and the step, as discussed in section 3.2. Note that for NO adsorbed at the on-top site at the step, the Pt-N bond is in a direction almost perpendicular to the step facet, while the N-O bond is considerably tilted away from the Pt-N bond, as can be seen from Fig. 5 (a). In the case of NO adsorbed at the on-top site of the flat Pt(111) surface [11,12], the Pt-N bond is almost perpendicular to the surface, while the N-O bond is greatly tilted from the surface normal. However, the occupation of on-top sites at steps occurs only when the local coverage at steps is high.

Although the adsorption sites near the step on the upper terrace are rather stable, those on the lower terrace are not. This may be due to the Pauli repulsion between the NO molecule and the step facet. At 11 K, our previous IRAS study reported that a weakly chemisorbed species near the step was observed at 1385 cm^{-1} [31]. This species could be assigned to the hcp-hollow NO on the lower terrace near the step; this species disappears when heated to 70 K.

4 Conclusion

In this study, we elucidated the adsorption states of NO on the Pt(111) step surface by using IRAS, STM and DFT calculations. On the (111) terrace, we observed that NO molecules were adsorbed at fcc hollow, hcp hollow and on-top sites. On the other hand, on the step, the stretching mode of the NO is observed at 1630 cm^{-1} . In addition, our DFT calculations also show that the stretching frequency is 1607 cm^{-1} and a bridge site is the most stable for NO.

Furthermore, we directly confirm that NO molecules adsorb at the two-fold bridge sites of the step by STM.

Acknowledgements

This work was partly supported by the Toray Science Foundation. One of the authors (N.T.) wishes to acknowledge the support of the JSPS (Japan Society for the Promotion of Science) Research Fellowship for Young Scientists. Aizawa acknowledges a visiting professorship of ISSP in 2003.

References

- [1] W. A. Brown, D. A. King, *J. Phys. Chem. B* 104 (2000) 2578
- [2] H. Ibach, S. Lehwald, *Surf. Sci.* 76 (1978) 1
- [3] J. L. Gland, B. A. Sexton, *Surf. Sci.* 94 (1980) 355
- [4] B. E. Hayden, *Surf. Sci.* 131 (1983) 419
- [5] M. Kiskinova, G. Pirug, H. P. Bonzel, *Surf. Sci.* 136 (1984) 285
- [6] N. Materer, A. Barbieri, D. Gardin, U. Starke, J. D. Batteas, M. A. Van Hove, G. A. Somorjai, *Surf. Sci.* 303 (1994) 319
- [7] N. Materer, A. Barbieri, D. Gardin, U. Starke, J. D. Batteas, M. A. Van Hove, G. A. Somorjai, *Phys. Rev. B* 48 (1993) 2859
- [8] Q. Ge, D. A. King, *Chem. Phys. Lett.* 285 (1998) 15
- [9] M. Matsumoto, N. Tatsumi, K. Fukutani, T. Okano, T. Yamada, K. Miyake, K. Hata, H. Shigekawa, *J. Vac. Sci. Technol. A* 17 (1999) 1577
- [10] M. Matsumoto, K. Fukutani, T. Okano, K. Miyake, H. Shigekawa, H. Kato, H. Okuyama, M. Kawai, *Surf. Sci.* 454 (2000) 101
- [11] M. Matsumoto, N. Tatsumi, K. Fukutani, T. Okano, *Surf. Sci.* 513 (2002) 485
- [12] H. Aizawa, Y. Morikawa, S. Tsuneyuki, K. Fukutani, T. Ohno, *Surf. Sci.* 514 (2002) 394
- [13] J. F. Zhu, M. Kinne, T. Fuhrmann, R. Denecke and H. P. Steinruck, *Surf. Sci.* 529 (2003) 384
- [14] K. Irokawa, H. Arai, J. Kobayashi, T. Kioka, S. Sugai, H. Miki and H. Kato, *Surf. Sci.* 357-358 (1996) 274
- [15] V. K. Agrawal, M. Trenary, *Surf. Sci.* 259 (1991) 116

- [16] Z. P. Liu, S. J. Jenkins, D. A. King, *J. Am. Chem. Soc.* 125 (2003) 14660
- [17] T. Sugisawa, J. Shiraishi, D. Machihara, K. Irokawa, H. Miki, C. Kodama, T. Kuriyama, T. Kubo, H. Nozoye, *App. Surf. Sci.* 169-170 (2001) 292
- [18] R. J. Mukerji, A. S. Bolina, W. A. Brown, *J. Chem. Phys.* 119 (2003) 10844
- [19] R. J. Mukerji, A. S. Bolina, W. A. Brown, *J. Phys. Chem. B* 108 (2004) 289
- [20] E. H. G. Backus, A. Eichler, M. L. Grecea, A. W. Kleyn, M. Bonn, *J. Chem. Phys.* 121 (2004) 7946
- [21] I. Villegas, R. Gomez, M.J. Weaver, *J. Phys. Chem.* 99 (1995) 14832
- [22] J. Yoshinobu, M. Kawai, *Chem. Lett.* (1995) 605
- [23] P. Hollins, J. Pritchard, *Prog. Surf. Sci.* 19 (1985) 275
- [24] J. Yoshinobu, N. Tsukahara, F. Yasui, K. Mukai, and Y. Yamashita, *Phys. Rev. Lett.* 90 (2003) 248301
- [25] Y. Morikawa, *Phys. Rev. B* 63 (2001) 033405, and references therein.
- [26] J.P. Perdew, K. Burke, M. Ernzerhof, *Phys. Rev. Lett.* 77 (1996) 3865.
- [27] D. Vanderbilt, *Phys. Rev. B* 41 (1990) 7892.
- [28] N. Troullier, J.L. Martins, *Phys. Rev. B* 43 (1991) 1993.
- [29] B. Hammer, *Phys. Rev. Lett.* 83 (1999) 3681. and references therein.
- [30] This value is somewhat different from that calculated for NO adsorbed at the fcc-hollow site of the (111) flat surface (2.09 eV) [12]. The difference is considered to be derived from that in the coverage of NO. In the reference [12], the calculation was performed using a p(2x2) unit cell, and therefore the coverage of NO was 1/4 ML. In the present case, on the other hand, the coverage of NO is as low as 1/12 ML. Thus the interaction between the NO molecules is much weaker in the present case than in that of the reference [12]. As can be seen from the fact that NO molecules tend to form dimers in the gas phase, the interaction between the NO molecules is attractive. That is why the surface with a larger coverage of NO is more stabilized, resulting in higher adsorption energy.
- [31] N. Tsukahara, K. Mukai, Y. Yamashita, J. Yoshinobu, *Surf. Sci.* in press
- [32] W. A. Brown, R. K. Sharma, and D. A. King, *J. Phys. Chem. B* 102 (1998) 5303
- [33] W. A. Brown, R. K. Sharma, Q. Ge, and D. A. King, *Phys. Chem. Chem. Phys.* 1 (1999) 1995

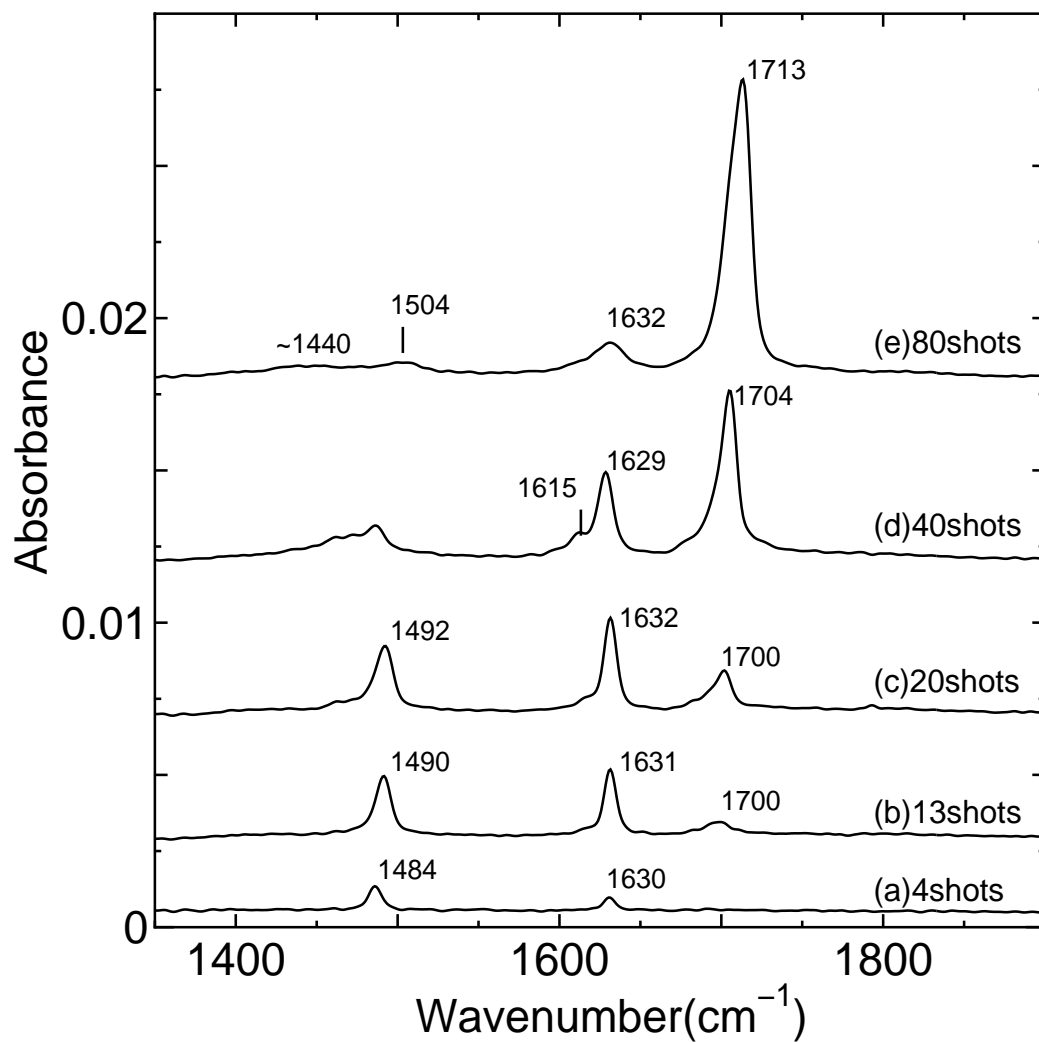


Fig. 1. IRAS spectra of NO on Pt(997) as a function of coverage. NO exposure and IRAS measurements were all carried out at 90 K. When the valve of a gas line was opened once (= 1 shot), a certain amount of NO gas was introduced to the clean Pt(997) surface, which corresponds to the coverage of 0.02 ML. All IRAS spectra were taken with a resolution of 4 cm^{-1} and 500 scans.

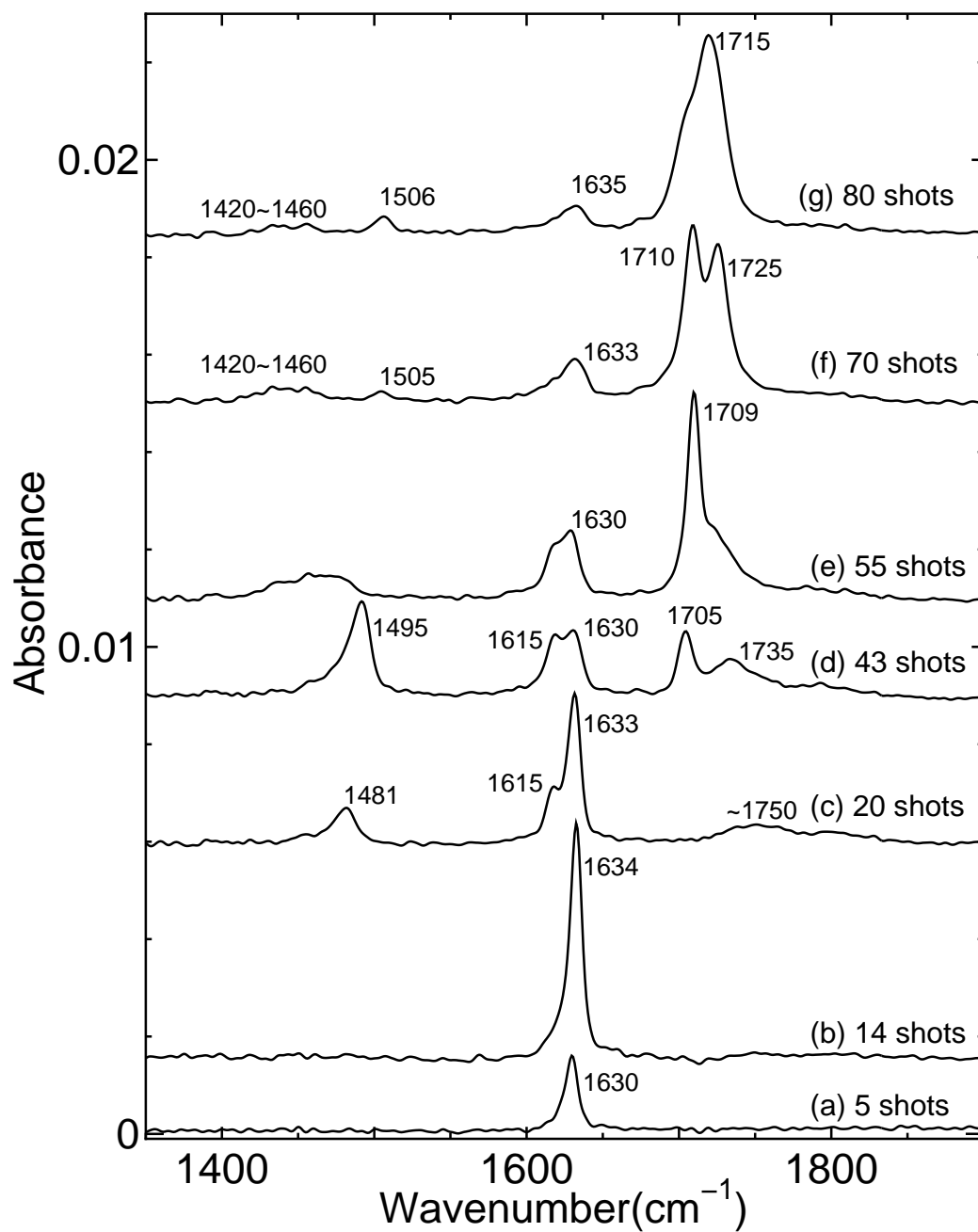


Fig. 2. IRAS spectra of NO on Pt(997) as a function of coverage. NO exposure and IRAS measurements were all carried out at 140 K. When the valve of a gas line was opened once (= 1 shot), the coverage of NO on Pt(997) was about 0.01 ML.

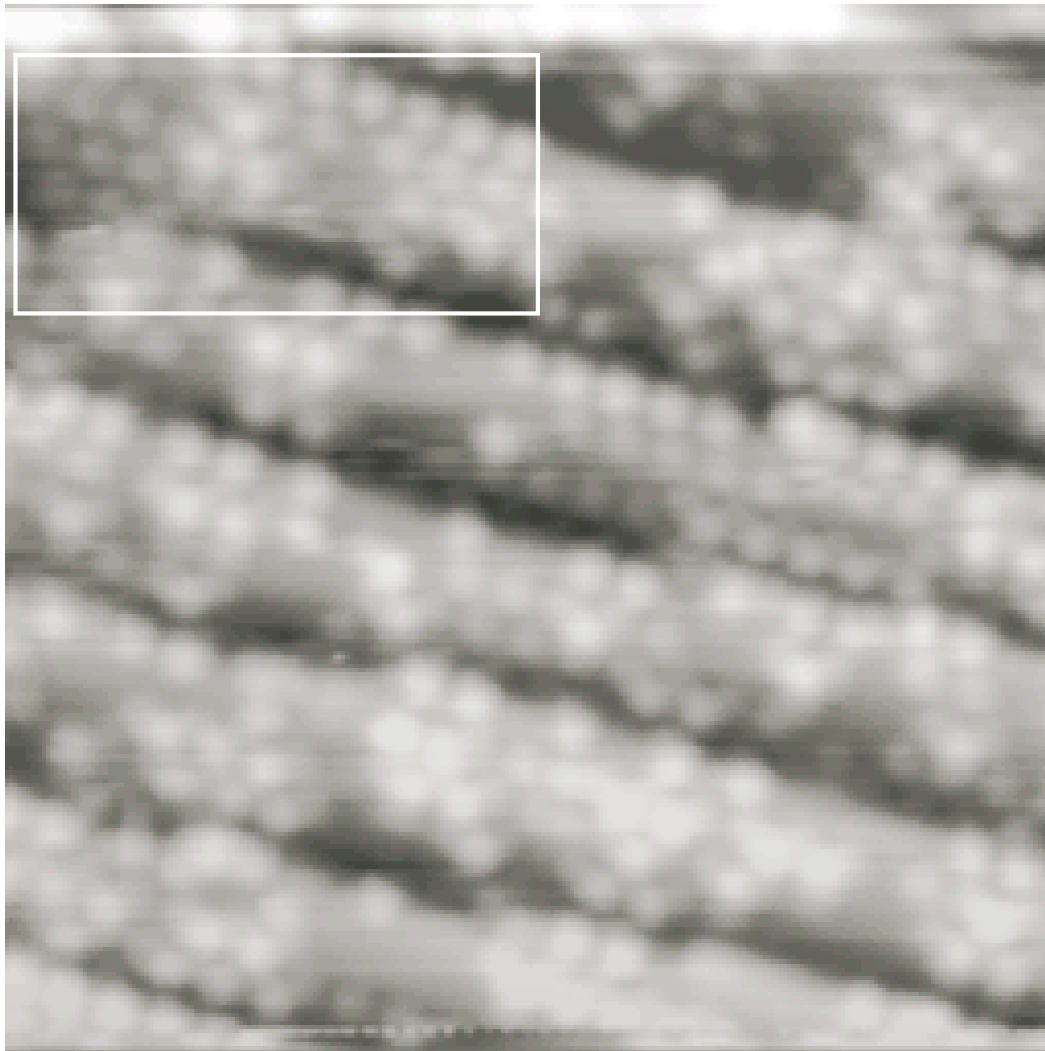


Fig. 3. An STM image of NO on Pt(997) at 86 K. $V_S = -0.1\text{V}$, $I_t = 0.2\text{nA}$. $11 \times 11 \text{ nm}^2$

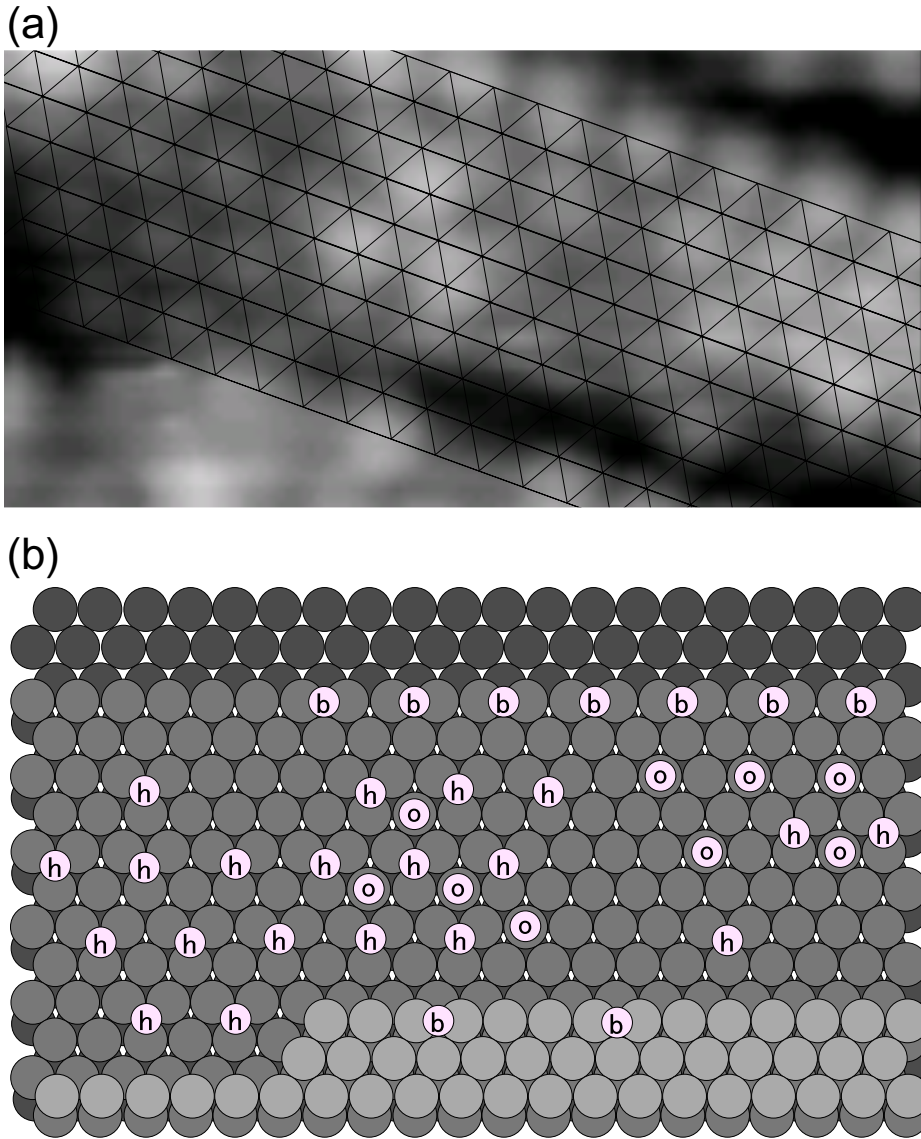
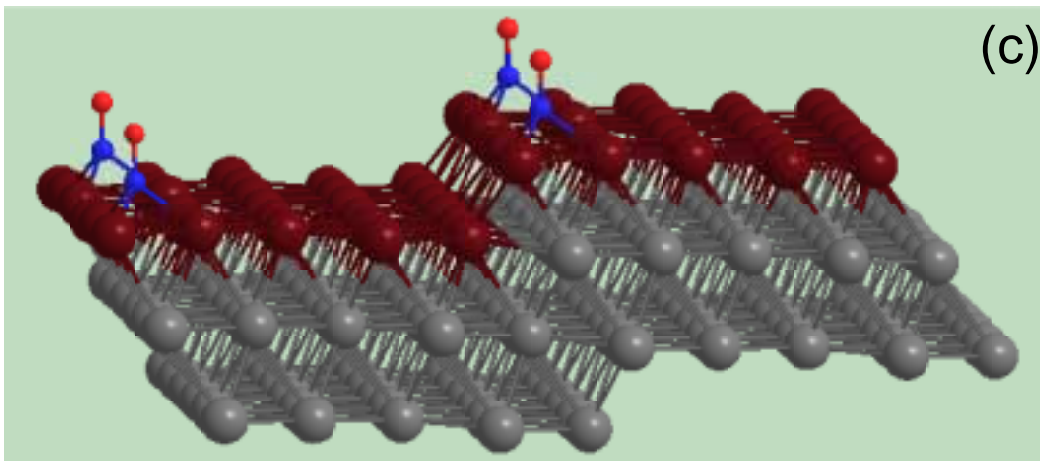
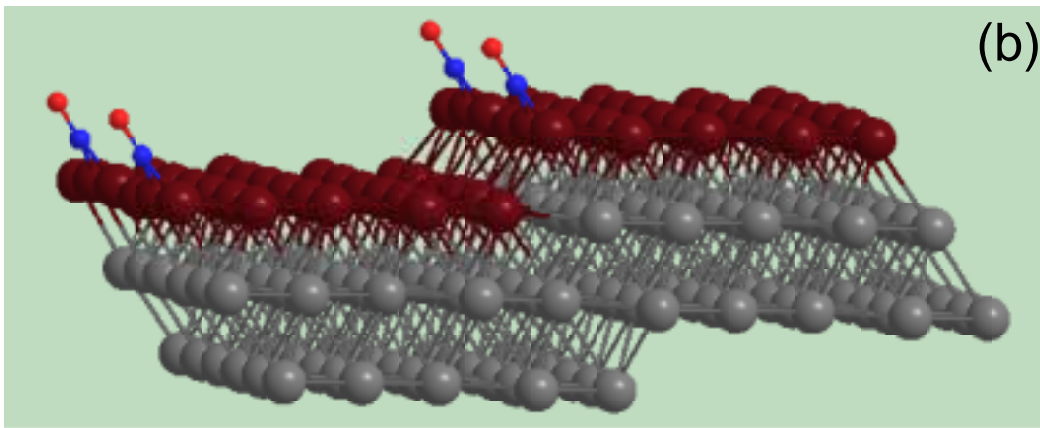
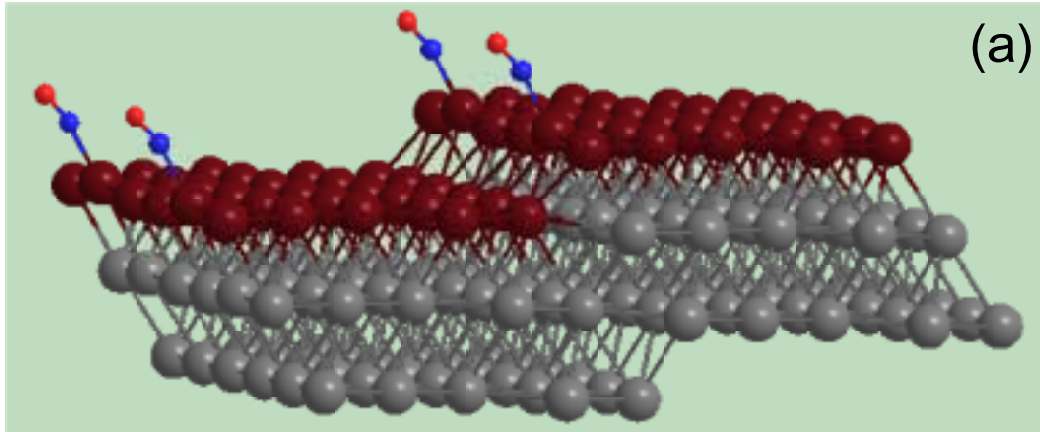


Fig. 4. (a) The enlarged image of the rectangle in Fig. 3. The center of the protrusion of NO at the step is located between two Pt atoms. (b) The proposed adsorption model; gray circles are Pt atoms, white circles are NO molecules. The labels on the white circles indicate the NO adsorption site: "b" is bridge, "o" is on-top and "h" is hollow.



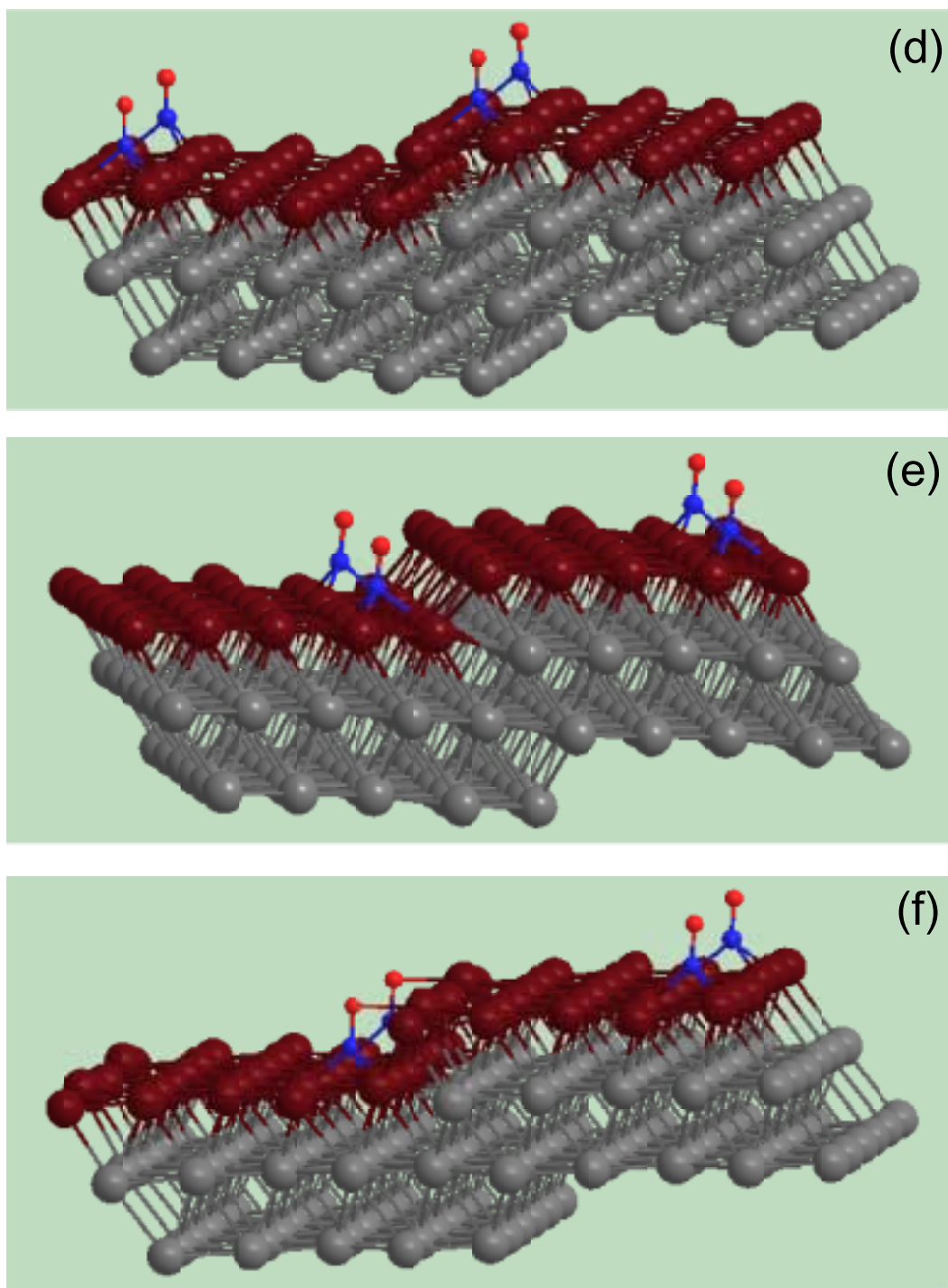


Fig. 5. The atomic structures of NO molecules adsorbed near the steps of the Pt(553) surface. The red and blue spheres represent O and N atoms, respectively. The brown and grey spheres represent Pt atoms at the surface and sub-surface layers, respectively. The adsorption sites of NO are as follows: (a) the on-top site on the upper terrace (b) the bridge site on the upper terrace (c) the fcc-hollow site on the upper terrace (d) the hcp-hollow site on the upper terrace (e) the fcc-hollow site on the lower terrace (f) the hcp-hollow site on the lower terrace.

Adsorption site	Adsorption energy [eV]	N-O stretching frequency [cm^{-1}]	Figure
on-top (upper)	2.03	1683	(a)
bridge (upper)	2.49	1607	(b)
fcc-hollow (upper)	2.15	1474	(c)
hcp-hollow (upper)	1.89	1506	(d)
fcc-hollow (lower)	1.62	1471	(e)
hcp-hollow (lower)	0.87	1188	(f)

Table 1

The adsorption energy and N-O stretching frequency calculated for six adsorption sites of NO near the step edge. In the column "Adsorption site", "(upper)" and "(lower)" represent adsorption sites on the upper and lower terraces, respectively. The adsorption geometries are illustrated in Fig. 5(a)-(f) according to the column "Figure".